View metadata, citation and similar papers at core.ac.uk
brought to you by CORE
provided by National Institute of Polar Research Repository

Antarct. Meteorite Res., **11**, 178–188, 1998

MAGNETIC CONTAMINATIONS OF SMALL IRON METEORITES, ODESSA AND GIBEON

Tetsuya FUKUHARA[1], Minoru FUNAKI[2] and Hiroyuki NAGAI[1]

[1]*Department of Physics, Faculty of Science, Shinshu University, 1–1, Asahi 3-chome, Matsumoto 390-0802*
[2]*National Institute of Polar Research, 9–10, Kaga 1-chome, Itabashi-ku, Tokyo 173-8515*

Abstract: Small samples of Odessa iron meteorites and Gibeon iron meteorites were studied to assess any magnetic contaminations acquired after the meteorites reached the surface of the earth. Odessa showed a stable component of natural remanent magnetization (NRM) present during AF demagnetization up to 50 mT. The NRM intensity decreased from one side to the other side with the exception of an interior sample. These variations in NRM might be acquired by artificial magnetic contamination, which is supported by the REM (the ratio of NRM to saturation isothermal remanent magnetization (SIRM)) value proposed by WASILEWSKI and DICKINSON (1998). The Gibeon's subsample directions with stronger NRM intensities made one cluster and those weaker intensities clustered at a different site. According to the REM values, the more intense NRM's might be the result of a magnetic contamination overprint. From these experimental subsamples analyses, from small iron meteorites, we find that the possibility of magnetic contamination must be considered during NRM analyses of meteorite magnetism.

1. Introduction

Magnetic properties of iron meteorites provide basic information about the physical properties of meteorites and may also give us paleomagnetic information that is relevant to understanding the thermo physical history of the parent body. Understanding the natural remanent magnetization (NRM) is the important first step in evaluating the magnetic properties of iron meteorites. KUKKONEN and PESONEN (1983) reported variable NRM intensity ranging from 10^{-4} to 10^{-1} Am^2/kg in 9 iron meteorites. PESONEN *et al.* (1993) reported an average NRM intensity of 2.06×10^{-2} Am^2/kg for 131 iron samples. Their NRM intensities were not screened for magnetic contaminations. The NRM for iron meteorites may include some component due to contaminations. Occasionally a hand magnet might be come into contact with the iron to check whether it is a meteorite or not. In a worst case scenario, a strong magnet might be used in a search for iron meteorites. These resultant magnetic contaminations might be responsible for some of the variation of NRM, observed by KUKKONEN and PESONEN (1983) and PESONEN *et al.* (1993).

Antarctic meteorites as well as lunar rocks returned by Apollo missions were collected carefully to avoid any chemical and magnetic contaminations. Extremely weak NRM (1.18×10^{-6} Am^2/kg) was reported for Yamato-75031 a small Antarctic iron meteorite (60.2 g) by NAGATA (1979). He estimated that the weak NRM was due to heating above the Curie point in the earth's atmosphere. This is another source of contamination in small meteorites.

In order to assess of the role of magnetic contamination in iron meteorites, small samples of Odessa (31.14 g) and Gibeon (60.28 g) were obtained from a dealer. Each shape was irregular with a rough surface. Any fusion crust and severe oxide appeared to have been removed from the surface of Odessa but for Gibeon a reddish brown crust layer remained on the surface, this crust was less than 1 mm thick, and it was difficult to evaluate if this may have been part of an original fusion crust.

Odessa is an inclusion-rich coarse octahedrite with a structure typical of group IA irons with Widmanstätten band width 1.70±0.25 mm. Odessa analyzes as 7.35 wt% Ni, 0.48 wt% Co and 0.25 wt% P (BUCHWALD, 1975). Gibeon is classified as a group IVa polycrystalline fine octahedrite with a Widmanstätten bandwidth 0.30±0.05 mm. Gibeon analyzes as 7.93 wt% Ni, 0.41 wt% Co and other minor elements (BUCHWALD, 1975).

2. Experimental Results

2.1. Natural remanent magnetization

Strips about 2 mm thick were cut perpendicular to the elongated shape of the bulk meteorite. Subsequently, 6 and 8 cubic subsamples of 0.0191 to 0.268 g in weight all with mutual orientation were cut from the respective strips from Odessa and Gibeon. Some subsamples of Odessa contained silicate or sulfide inclusions but none were seen

Table 1. NRM of the subsamples for Odessa and Gibeon.

	Weight (g)	Distance (cm)	NRM ($10^{-2}Am^2/kg$)	I (degree)	D (degree)	REM (NRM/SIRM)
Odessa						
A1	0.0295	0	36.20	50.3	305.9	0.593
A2	0.0426	0.33	23.41	−4.8	181.7	0.384
A3	0.0961	0.61	9.71	14.2	257.3	0.159
A4	0.0701	0.99	17.41	3.2	237.7	0.285
A5	0.0690	1.22	3.47	43.5	346.8	0.057
A6	0.0191	1.41	3.33	50.3	133.9	0.055
BRECHER and ALBRIGHT (1977)			0.62*			0.010
DuBOIS (1965)			~0.087			0.001
GUSKOVA (1970)			2.2–1.8			0.036–0.030
Gibeon						
B1	0.195	0	7.13	−7.3	60.1	0.162
B2	0.268	0.38	3.18	−17.1	51.4	0.072
B3	0.202	0.60	2.26	−15.2	42.9	0.051
B4	0.196	0.84	1.45	−33.2	64.5	0.033
B5	0.196	1.13	1.47	6.3	83.3	0.033
B6	0.184	1.38	1.67	35.6	89.8	0.038
B7	0.164	1.60	1.23	27.0	93.1	0.028
B8	0.099	1.95	2.85	7.3	28.3	0.065
BRECHER (1972)			2.75			0.063
GUSKOVA (1965)			36–3.3			0.820–0.075

*Density was assumed to ρ=7.0 in this study.

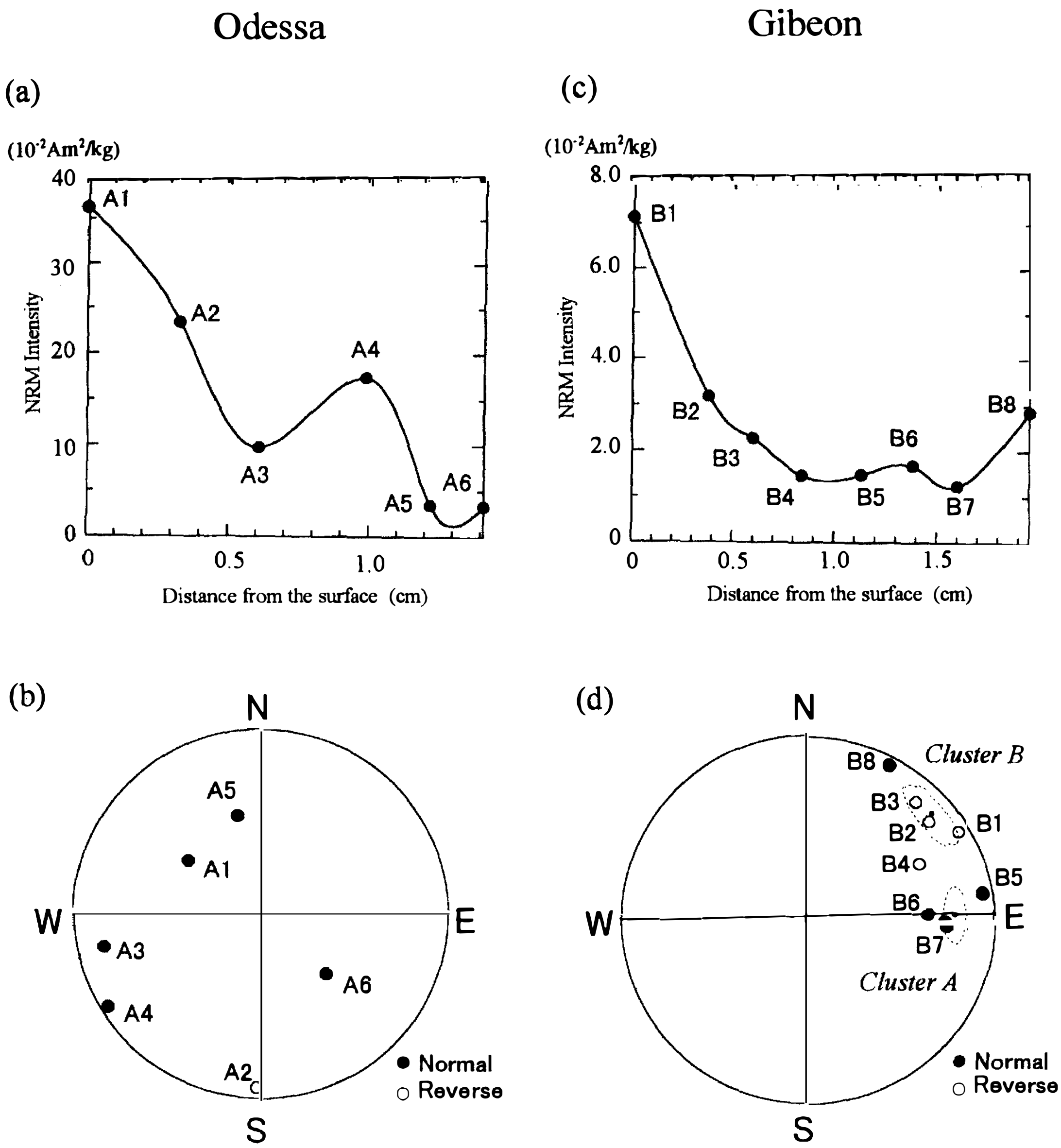

Fig. 1. Variation of NRM intensity of subsamples for Odessa (a) and Gibeon (c), and the distribution of their directions for Odessa (b) and Gibeon (d). The α_{95} values of the Cluster A and B are shown in (d) by dotted ellipses.

in the Gibeon subsamples. The subsamples were numbered from one side of the surface to the other side as A1 to A6 for Odessa and B1 to B8 for Gibeon. A1, A6, B1 and B8 therefore include the sample surface.

The NRM intensities (between 36.2×10^{-2} and 3.33×10^{-2} Am^2/kg) for Odessa subsamples were inhomogeneous (Table 1). Subsample A1 had the largest magnetization intensity and A6 carried the smallest one. The intensities decreased from A1 to A3, but A4 was anomalously large otherwise of a smooth intensity-distance curve from surface to surface was observed, as shown in Fig. 1a. The NRM directions of these subsamples (Fig. 1b) were scattered as supported by the confidence angle of 95% prob-

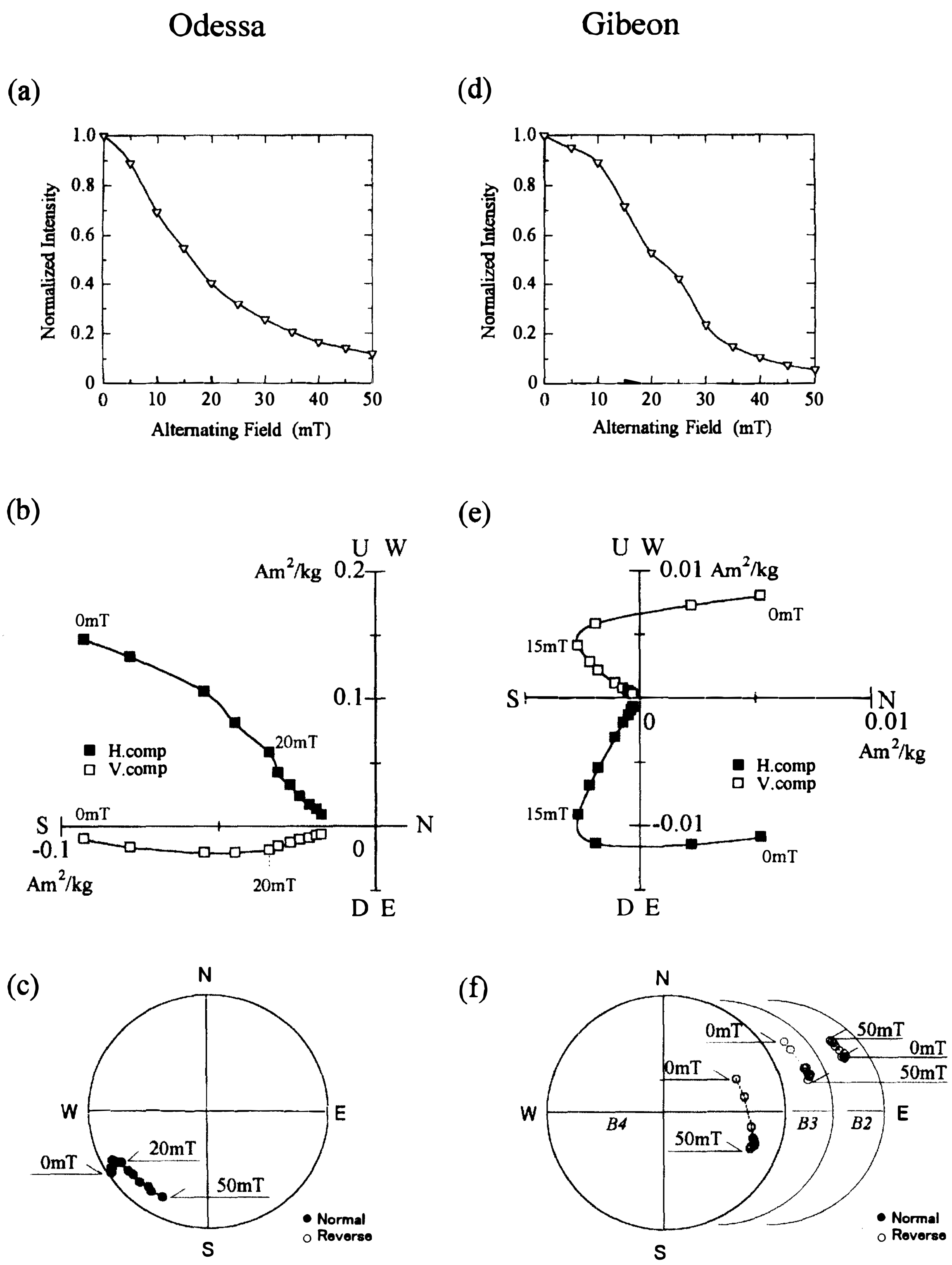

Fig. 2. AF demagnetization curves of Odessa and Gibeon: variations of respective NRM intensity (a, d), Zijderveld projections (b, e) and direction (c, f).

ability (α_{95})=68.9° and precision parameter (k)=1.9.

The NRM intensity of subsamples for Gibeon ranged from 7.13×10^{-2} for B1 to 1.23×10^{-2} Am^2/kg for B7 (Table 1). NRM intensity steeply decreased from B1 to B2, and then varied gradually, as shown in Fig. 1c. Their NRM directions appear to group into Cluster, A and B, as shown in Fig. 1d; Cluster A consists of the interior samples (B5, B6 and B7), while the Cluster B consists of mixture from the interior (B2, B3, B4) and surface (B1, B8) samples. The confidence and precision parameter were obtained as α_{95}=9.5° and k=26.6 for Cluster A and α_{95}=13.6° and k=16.1 for Cluster B.

2.2. AF and thermal demagnetization

Subsamples A3, A4 and A6 (Odessa) and B2, B3 and B4 (Gibeon) were demagnetized in alternating fields (AF demagnetization) up to 50 mT with steps of 5 mT. Figure 2 shows typical representations of AF demagnetization curves for intensity, direction and component behavior (Zijderveld projection) for Odessa (A4) and Gibeon (B4). Subsample A4 showed gradually decreasing intensity from an initial 17.41×10^{-2} to 2.07×10^{-2} Am^2/kg at 50 mT (Fig. 2a). There was little directional shift between 0 mT and 20 mT but the direction shifts southward between 20 mT and 50 mT as shown Fig. 2b and c. This characteristic of demagnetization was essentially consistent among the subsamples.

Gibeon B4 NRM, whose intensity was 1.45×10^{-2} Am^2/kg, demagnetized in steps with curve slopes changing at 10, 20 and 30 mT. The final intensity was 8.09×10^{-4} Am^2/kg at 50 mT (Fig. 2d). The direction shifts toward southeastward between 0 mT and 15 mT (Fig. 2e and f). There was little directional shift between 15 mT and 50 mT. The NRM for B2 and B3 showed more directional stability than B4, and the intensity decreased more gradually.

Subsamples of Odessa (A1, A2 and A5) and Gibeon (B5, B6 and B7) were enclosed in glass capsules under 10^{-1} Pa pressure for thermal demagnetization up to 630°C using steps of 50°C. Typical results of the demagnetization are shown in Fig. 3 for A5 and Fig. 4 for B5. The NRM intensity of A5 (3.47×10^{-2} Am^2/kg) was gradually thermally demagnetized to 7.17×10^{-4} Am^2/kg at 630°C with a clearly defined unblocking temperatures (UBT) at 580°C (Fig. 3a). Although small zigzag variations appeared in the horizontal component between 30°C and 230°C (Fig. 3c), there is no large directional change up to 580°C (Fig. 3b). The magnetization direction was unstable beyond 580°C. The demagnetization curves for A1 and A2 showed UBT's at 330°C and 580°C (Fig. 3a). The low temperature components of A1 and A2 NRM's were more unstable than the high temperature one against thermal demagnetization. Subsequently, subsample A5 which was heated to 630°C was subjected to a 0.1 T magnetic field by touching it with a ferrite-magnet in order to impart an isothermal remanent magnetization (IRM). The IRM was then thermally demagnetized under the same conditions. The intensity (6.58×10^{-2} Am^2/kg) decreased gradually to 2.88×10^{-3} Am^2/kg at 630°C with 2 UBT's at 330° and 580°C (Fig. 3a). The IRM component contamination showed no special directional changes throughout the demagnetization (Fig. 3b and d).

The NRM (1.47×10^{-2} Am^2/kg) of Gibeon subsample B5 was thermally demagnetized to 3.62×10^{-5} Am^2/kg at 630°C with the clearly defined UBT at 530°C (Fig. 4a).

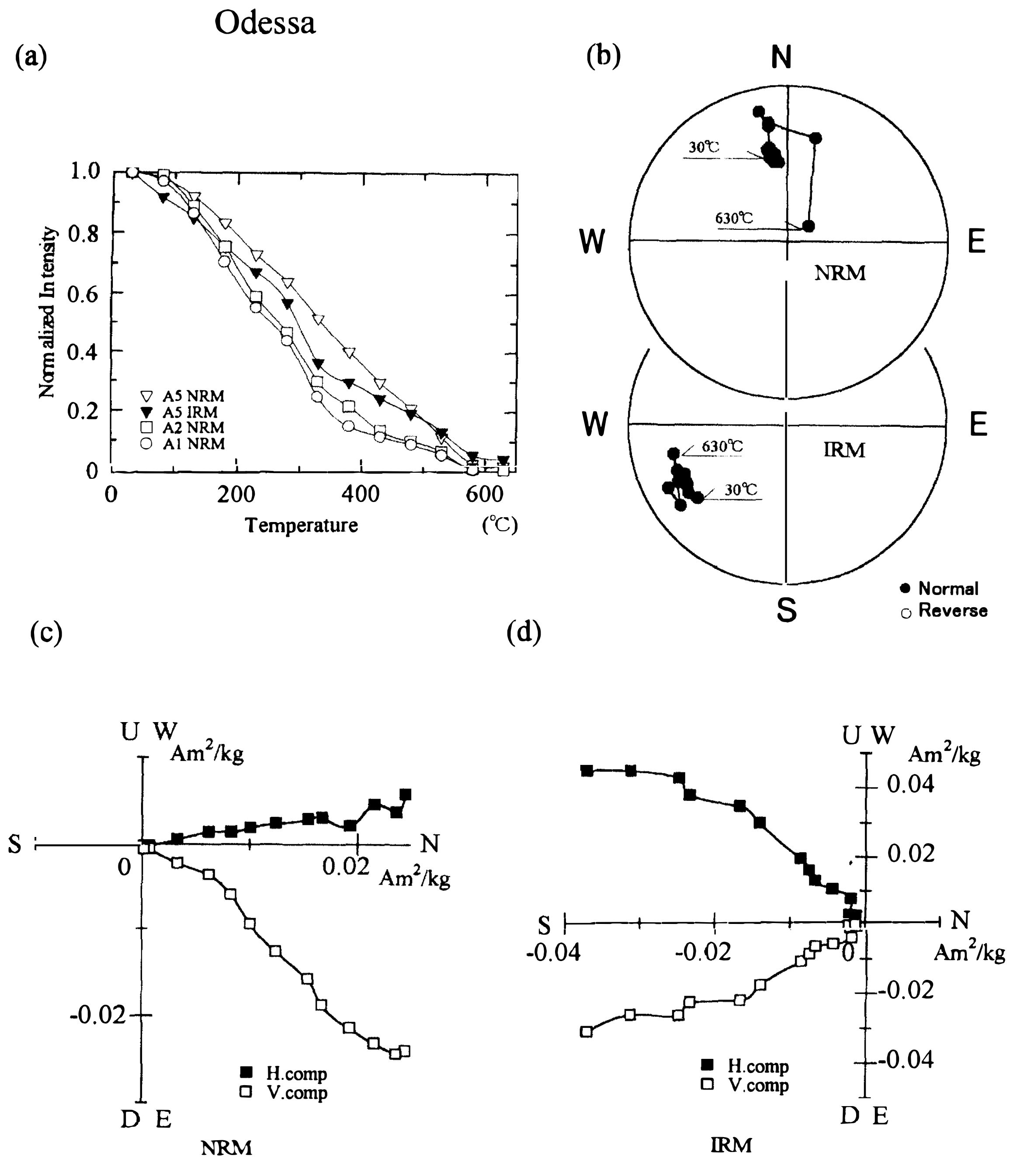

Fig. 3. Thermal demagnetization curve results for NRM and IRM in Odessa. (a) NRM intensity curve for 3 subsamples in A1, A2 and A3 (open symbols) and IRM curve for A5 (solid symbol). IRM was acquired in after touching the A5 sample which had been probably heated to 630°C. The estimated contamination field is 0.1T. (b) directional change of NRM and IRM. (c) and (d) Zijderveld projection of NRM and IRM for A5 respectively.

The NRM direction was restricted to a limited area between 30°C and 480°C although small zigzag variations appeared in the horizontal component between 30°C and 330°C (Fig. 4b and c). The direction was unstable beyond 530°C. The other 2 subsamples showed almost the same characteristics of thermal demagnetization as illustrated by B5.

The heated subsample B5 was also given an IRM by touching it with the magnet. The IRM intensity (3.93×10^{-2} Am^2/kg) was thermally demagnetized to 1.19×10^{-3} Am^2/kg at 630°C with the clearly defined UBT at 380° and 630°C (Fig. 4a). The IRM horizontal components zigzagged up to 380°C, and then it stabilized as shown in the Zijderveld diagram (Fig. 4d). The IRM thermal demagnetization curve was very different from that of the NRM. These demagnetization properties were very similar for all other subsamples (B6 and B7).

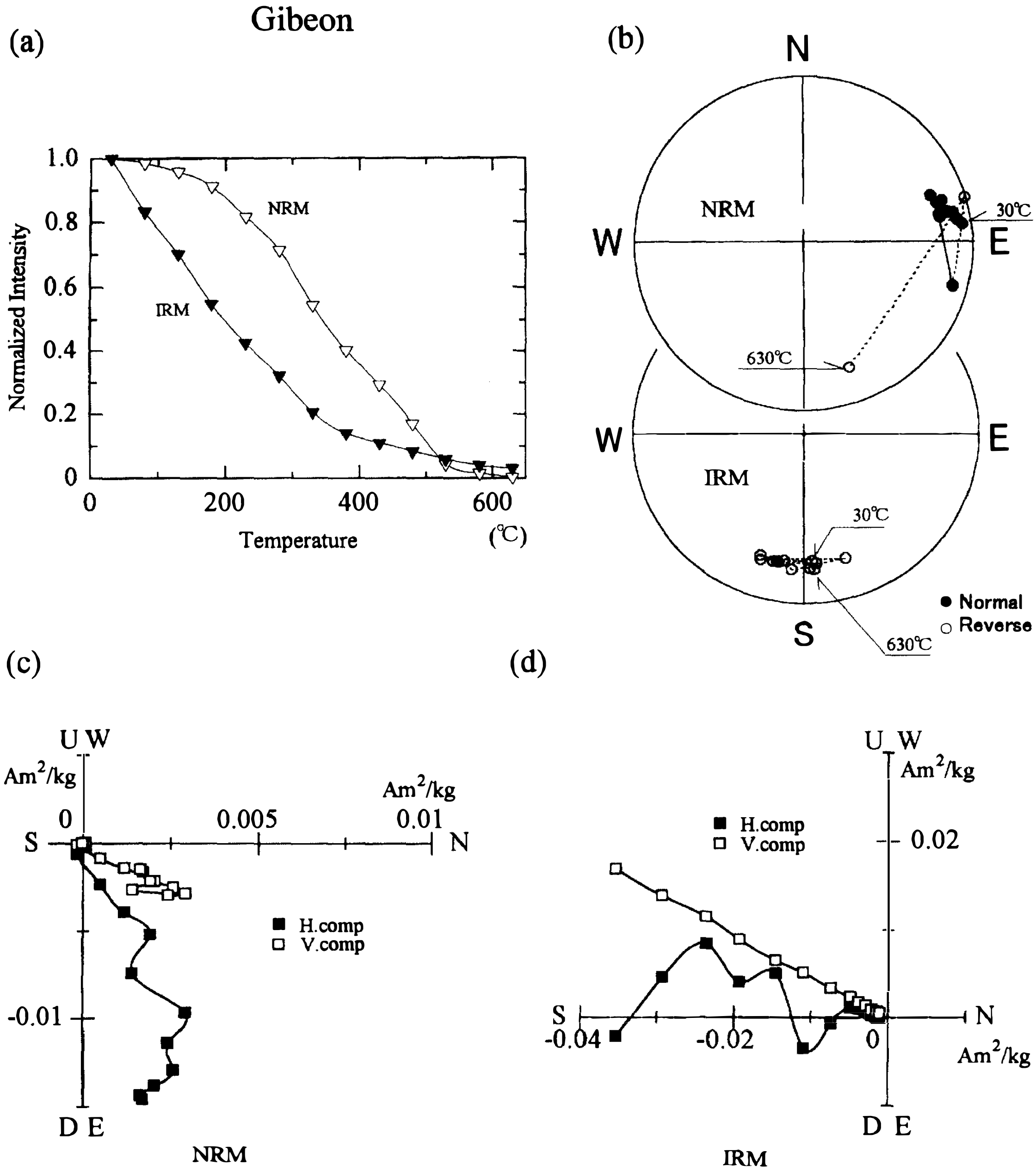

Fig. 4. Thermal demagnetization curves of NRM and IRM of the Gibeon subsample B5. (a) intensity demagnetization curve of NRM and IRM. (b) directional change of NRM and IRM. (c) and (d) Zijderveld projection of NRM and IRM for B5 respectively.

2.3. Thermomagnetic curve (Is-T curve) and hysteresis properties

Thermomagnetic (*Is-T*) curves were obtained using a vibrating sample magnetometer (VSM). Measurements were made from room temperature to 820°C under 10^{-3} Pa pressure in an external steady magnetic field of 1.0 T. The heating and cooling rates were 200°C/h. The *Is-T* curve of Odessa, Fig. 5a, was irreversible with the phase transition (*Tc*) from kamacite (α-phase) to taenite (γ-phase) at $Tc_{\alpha\rightarrow\gamma}$ =700°C in the heating curve and from taenite to kamacite at $Tc_{\gamma\rightarrow\alpha}$ =550°C in the cooling curve. The spontaneous magnetization of 156 Am^2/kg at room temperature did not drastically change (161 Am^2/kg) after heat treatment. As the *Is* value of pure iron is 210 Am^2/kg, the amount of kamacite in Odessa is estimated to be 74.3%, with adjustment for 6.2% Ni in the kamacite.

The *Is-T* curve of Gibeon (Fig. 5b) showed $Tc_{\alpha\rightarrow\gamma}$ =720°C in the heating curve and $Tc_{\gamma\rightarrow\alpha}$ =550°C in the cooling curve, suggesting kamacite with 6.0%Ni for the magnetic mineral. Since the original magnetization (204 Am^2/kg) decreased to 197 Am^2/kg after heating, some chemical or physical alterations might have occurred.

The magnetic hysteresis properties were also measured with the VSM, at room temperature, using an external magnetic field of 1.5 T. The results are summarized in Table 2. The saturation magnetization (*Is*) of Odessa and Gibeon were calculated to be 149 and 209 Am^2/kg respectively. The coercive force (*Hc*) was very small, less than 0.83 mT, suggesting multi-domain structure.

Table 2. Magnetic hysteresis properties of Odessa and Gibeon.

	Odessa	Gibeon
Saturation magnetization, *Is* (Am^2/kg)	149	209
Saturation remanence, I_R (Am^2/kg)	0.610	0.439
Coercive force, *Hc* (mT)	0.83	0.5

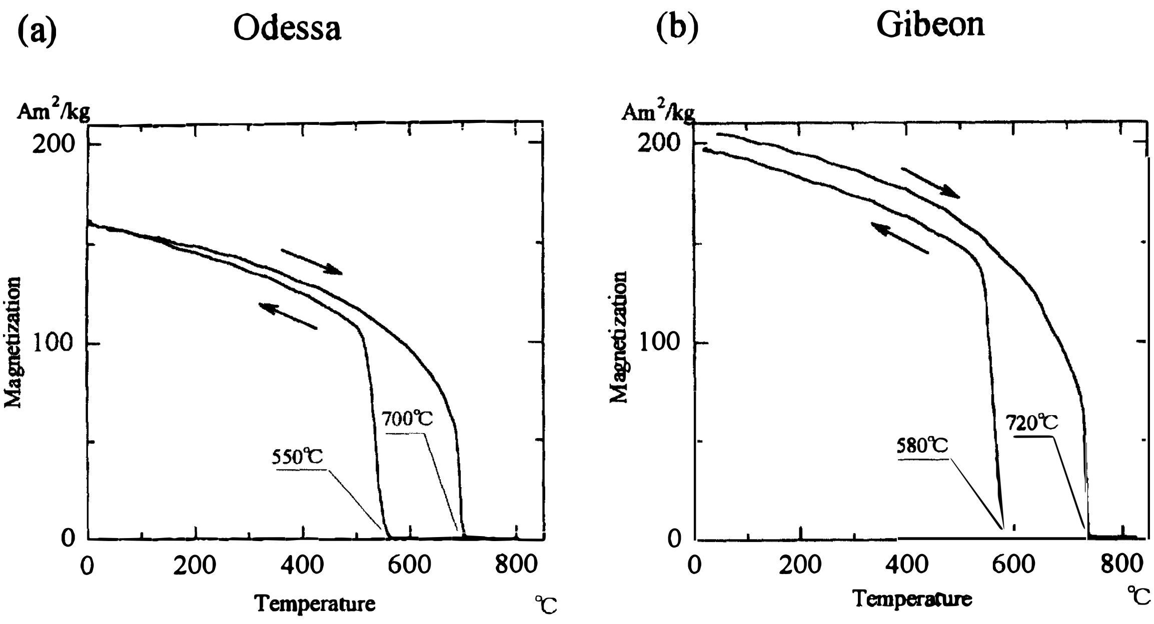

Fig. 5. Thermomagnetic curves of the 1st run cycle for Odessa (a) and Gibeon (b) in a steady external magnetic field of 0.1 T under 10^{-3} Pa atmospheric pressure.

3. Discussion

The principal magnetic mineral in Odessa is identified to be kamacite with 6.2%Ni, this was estimated from the phase transition temperatures in the *Is-T* curve. It has been reported that the Ni content in kamacite is 7.35% in the bulk chemical analysis by Buchwald(1975) and 7.29% in the electron probe microscope analysis by Brecher and Cutrera (1976). Although the magnetic estimate of 6.2%Ni reflects a lower Ni content compared to chemical analyses, it may be due to an impurity effect in kamacite or to differences of bulk or point analyses.

According to Brecher and Albright (1977), the unstable NRM intensity (4.34×10^{-2} emu/cc (0.62×10^{-2} Am^2/kg, assuming density=7.0)) of Odessa was demagnetized by 5 mT and the direction scattered widely throughout AF demagnetization up to 30 mT. Our sample carried both unstable and stable NRM components during the demagnetization. Although our NRM intensity is 3.47×10^{-2} Am^2/kg for A5 and 3.33×10^{-2} Am^2/kg for A6, these values are stronger than the NRM intensity measured by Brecher and Albright (1977). DuBois (1965) reported the NRM intensities from several samples of Odessa averaging $\sim0.087\times10^{-2}$ Am^2/kg. Our sample, at least A1, has a relatively strong NRM intensity which we infer to be due to magnetic contamination. The magnetic contamination of meteorites is suggested from REM values (the ratio of NRM to SIRM) by Wasilewski and Dickinson (1998). They report that typical REM values from a wide variety of natural materials and laboratory experiments show the REM is <0.05. And it is also reported that generally REM values >0.05 and certainly >0.01 indicate the sample has been contaminated by a hand magnet, lightning, or by some other process. As the SIRM of Odessa is I_R=0.439 Am^2/kg, the REM values varied from 0.08 to 0.82 for our subsamples, 0.01 for Brecher and Albright and 0.001 for DuBois (Table 1). Therefore, our subsamples A1 to A4 were considered to be contaminated magnetically in accordance with Wasilewski and Dickinson (1998). However, it is difficult to explain fully the variation of NRM intensities and directions among the subsamples by simple magnetic contamination, because they did not vary systematically. If a hand magnet touched Odessa, the subsamples should acquire remanent magnetization toward the same direction and the intensity would decrease with exponential inverse proportion. In Odessa the intensity of A4 is anomalous in the otherwise gradually decreasing trend and the NRM directions scattered widely for all subsamples as supported by large α_{95}=68.9° and small k=1.9 values. It is likely that the sample was touched with a magnet several times.

The thermal demagnetization curve of the NRM for A5 showed one UBT at 580°C, while that of the NRM for A1 and A2 (near the surface) showed UBT's at 330° and 580°C. The demagnetization curve of IRM after heating to 630°C for A5 showed UBT's at 330° and 580°C. This consistency of the UBT suggests that the NRM might have an IRM component. However since A5 was heated and then given an IRM we must determine if the heating altered the meteorite. A plausible scenario for the magnetic contaminations in our Odessa sample is as follows;

1) When Odessa entered the earth's atmosphere the meteorite was heated by the air friction and when the meteorite cooled down, TRM might be acquired. There is also a possibility of acquiring SRM when striking earth.
2) The possibility of acquiring CRM and/or VRM during long residence on earth is also

realistic. The influence of weathering should not be ignored.

3) Role of men who collect the meteorite. Some hunters of meteorites probably used a strong magnet in searching for meteorites. There is the possibility that the IRM was acquired at that time.

The magnetic mineral in Gibeon is identified as kamacite with 6%Ni from the *Is*-*T* curve, but kamacite with 7.93%Ni was reported from bulk chemical analysis (BUCHWALD, 1975). This Ni content inconsistency is explained as above for Odessa. The large saturation magnetization of Is=209 Am^2/kg suggests that the measured sample consists of kamacite without other phases.

The NRM intensity of Gibeon has been reported as 3.3×10^{-2}, 36×10^{-2} Am^2/kg (GUSKOVA, 1965) and 2.75×10^{-2} Am^2/kg (BRECHER, 1972). As the SIRM of Gibeon is given by I_R=0.439 Am^2/kg, no contamination is estimated for B4, B5, B6 and B7 (REM=0.03 to 0.04) by using the REM value. Subsamples B1, B2, B3 and B8 (REM= 0.05 to 0.16), Guskova samples (REM=0.8 to 0.06) and the Brecher sample (REM=0.06) suggest a wide REM range, including some with REM>0.1. Some of these are likely contaminated. There is a possibility that the strong magnetization intensities for B1 and B8 may be a TRM since they were near the fusion crust layer. However TRM will not give large REM values (WASILEWSKI and DICKINSON, 1998). The results of AF demagnetization showed small directional change within the Cluster B for B2 and B3, but the direction of the NRM component in B4 moved from Cluster B to Cluster A between 0 mT and 15 mT (Fig. 2f). The NRM intensity variations and the behavior of subsamples in Cluster B suggests that the magnetic contamination penetrated from B1 to B3.

The difference between NRM and IRM thermal demagnetization curves for B4 B5 and B6 of Gibeon may suggest that the subsamples, including the Cluster A, were not heated to more than 630°C during frictional heating in the earth's atmosphere. Namely, there is a possibility that some original NRM may survive in these subsamples since 630°C is lower than the $Tc_{\alpha\rightarrow\gamma}$ =720°C. The magnetic evidences from Gibeon suggests almost the same history of magnetic contamination as that described for Odessa.

In spite of low Hc value (0.5 mT) in Gibeon, the stable NRM component survived up to 60 mT AF demagnetization, as described by BRECHER (1972), and in this paper up to 50 mT. Further study should be done in order to solve how and where the stable NRM of Gibeon was acquired.

4. Concluding Remarks

The stable NRM component was observed in subsamples of Odessa, regardless their NRM intensities and directions varied. It is plausible that the NRM may contain a contamination overprint due to magnet touching, perhaps on several occasions. The fusion crust was likely removed by weathering or polishing before our measurements were done.

Gibeon has two different NRM direction clusters. The NRM directions, associated with strongest intensities, are found in exterior subsamples and those of weaker intensity are related to the interior of the small piece of Gibeon.

From these experimental results on small iron meteorites, the consideration of magnetic contaminations is rather important for analyses of meteorite magnetism. Probably most effective estimation of the presence of magnetic contamination is the REM value proposed by WASILEWSKI and DICKINSON (1998).

As indicated in WASILEWSKI and DICKINSON (1998) REM values due to TRM in most materials including Iron-Nickel alloy is <0.05. Large REM values suggest magnetic contamination or magnetization by some exotic mechanism like lightning.

Acknowledgments

The authors wish to thank Dr. P. WASILEWSKI, Goddard Space Flight Center, NASA, for reviewing the manuscript.

References

BRECHER, A. (1972): I. Vapor Condensation of Ni-Fe Phases and Related Problems. Ph.D. Thesis U.C.S.D.

BRECHER, A. and ALBRIGHT, L. (1977): The thermoremanence hypothesis and the origin of magnetization in iron meteorites. J. Geomagn. Geoelectr., **29**, 379–400.

BRECHER, A. and CUTRERA, M. (1976): A scanning election microscope (SEM) study of magnetic domain struc ture of iron meteorites and their synthetic analogues. J. Geomagn. Geoelectr., **28**, 31–45.

BUCHWALD, V.F. (1975): Handbook of Iron Meteorites. Vols. 1–3. Berkeley, Univ. Calif. Press, 1209 p.

DUBOIS, R.L. (1965): Some investigations of the remanent magnetism and domain structures of iron meteorites. J. Geomagn. Geoelectr., **17**, 381–390.

GUSKOVA, E.G. (1965): Study of natural remanent magnetization of iron and stony-iron meteorites. Geomagn. Aeron. V (transl), **1**, 91–96.

GUSKOVA, E.G. (1970): The magnetic properties of meteorites of the collection of the Committee for Meteorites of the USSR Academy of Sciences. Meteoritika, **30**, 74–87.

KUKKONEN, I. T. and PESONEN, L. J. (1983): Classification of meteorites by petrophysical methods. Geol. Soc. Finland, **55**, 2, 157–177.

NAGATA, T. (1979): Natural remanent magnetization of antarctic meteorites. Mem. Natl Inst. Polar Res., Spec. Issue, **12**, 238–249.

PESONEN, L. J., TERHO, M. and KUKKONEN, I. T. (1993): Physical properties of 368 meteorites: implications for meteorite magnetism and planetary geophysics. Proc. NIPR Symp. Antarct. Meteorites, **6**, 401–416.

WASILEWSKI, P. J. and DICKINSON, T. L. (1998): The role of magnetic contamination in meteorites. submitted to Meteoritics and Planetary Science.

(Received October 14, 1997; Revised manuscript accepted January 23, 1998)